Available online at www.sciencedirect.com
SCIENCE DIRECT
Mechatronics 16 (2006) 291–301
MECHATRONICS

Adaptive vehicle skid control

E. Faruk Kececi [a,*], Gang Tao [b]

[a] Department of Mechanical Engineering, Izmir Institute of Technology, Urla, Izmir 35430, Turkey
[b] Department of Electrical and Computer Engineering, University of Virginia, Charlottesville, VA 22903, USA

Received 21 September 2004; accepted 15 October 2005

Abstract

In this paper, adaptive vehicle skid control, for stability and tracking of a vehicle during slippage of its wheels without braking, is addressed. Two adaptive control algorithms are developed: one for the case when no road condition information is available, and one for the case when certain information is known only about the instant type of road surface on which the vehicle is moving. The vehicle control system with an adaptive control law keeps the speed of the vehicle as desired by applying more power to the drive wheels where the additional driving force at the non-skidding wheel will compensate for the loss of the driving force at the skidding wheel, and also arranges the direction of the vehicle motion by changing the steering angle of the two front steering wheels. Stability analysis proves that the vehicle position and velocity errors are both bounded. With additional road surface information available, the adaptive control system guarantees that the vehicle position error and velocity error converge to zero asymptotically even if the road surface parameters are unknown.

Keywords: Active steering control; Adaptive vehicle skid control; Driver assistance system; Non-linear adaptive control design; Vehicle stability and tracking

1. Introduction

Initially, active control of vehicle dynamic systems is used to reduce fuel consumption and emissions [1]. In current automotive technology, active control is also used to increase the safety and the reliability of the vehicle ride and handling. Special control systems are designed for different parts of the vehicle dynamics [2–4]. Anti-lock brake systems (ABS) are designed to prevent skidding of the wheels during braking [5,6], while traction control systems (TCS) are accomplishing the same objective, preventing the slipping of the wheels, during acceleration [6]. When the vehicle is on a slippery surface, because of the drop at the coefficient of road adhesion, the drive wheels may slip. The traction control system reduces the engine torque or applies brakes to the slipping wheels and brings the slipping wheels into the desirable skid range. In order to increase the stability of the vehicle during cornering, active yaw control systems are designed, where either by braking or by transferring the torque between the wheels, the speed of the vehicle is decreased to critical speed to turn the corner and yaw control is achieved [7,9,10]. Vehicle state estimation [11,12] and road condition estimation [13] methods are used to improve the performance of ABS, TCS and active yaw control systems. In [14–16] controller algorithms are designed to compensate for the error in the lateral and yaw motion where sliding mode control and minimization of cost function are used.

In order to increase the vehicle handling performance, advanced hardware designs are also used. In four-wheel steering vehicles, the rear wheels can also be steered [6,17] which increases the steering ability of the vehicle. The steer by wire mechanism which has replaced the conventional steering mechanism with electrical motors, rotates the steering wheels (which are the two front wheels

* Corresponding author. Tel.: +90 232 750 6618; fax: +90 232 750 6515.
E-mail addresses: farukkececi@iyte.edu.tr (E.F. Kececi), gt9s@virginia.edu (G. Tao).
URL: http://robotics.iyte.edu.tr (E.F. Kececi).

0957-4158/$ - see front matter © 2006 Elsevier Ltd. All rights reserved.
doi:10.1016/j.mechatronics.2005.10.005

of the vehicle) according to the driver's intentions [18–20]. This system gives the ability to implement the automatic steering concepts, which are used in driver assistance systems.

Direct yaw moment control systems, driver assistance systems, for vehicle handling at the high speed steering, are employed to stabilize the motion of the vehicle by braking the slipping wheel and bringing it to a skid range so that it can start applying driving force again [21]. These systems are used in applications such as lane change [14] and lane keeping [22].

In existing vehicle skid control systems, the skidding wheel is detected and the power applied to this wheel is reduced until the traction is regained. However, when the total vehicle dynamic is considered, after the skidding occurs, in order to regain control of the vehicle, the total speed of the vehicle is reduced, which can be a problem in traffic when it causes some vehicles to come to a sudden stop.

When a vehicle with an existing skid control technology is considered, where the total speed of the vehicle is decreased to regain traction at the skidding wheel, if the vehicles behind this slowing down vehicle do not need to slow down, because they do not need to have any traction problem, they can hit the slowing down vehicle. The biggest advantage of the proposed design is that it does not require for the vehicle to decrease its speed, so the vehicle will not cause any danger to the other vehicles in the traffic.

In this paper, the concept of controlling the stability of the vehicle during slippage of the wheels without braking, which can be applied to electrical vehicles [7] as well as the all wheel drive vehicles, where the drive wheels and steering wheels can be controlled separately, has been developed. An adaptive control algorithm is developed for the case when no road condition information is available. Stability analysis proves that the vehicle position and velocity errors are both bounded. If the additional road surface information available, the adaptive control system guarantees that the vehicle position error and velocity error converge to zero asymptotically even if the road surface parameters are unknown.

This research is the design of adaptive fault tolerant control algorithm. The application is the stability and tracking control of a vehicle and the failure is described as the slippage of the wheels of the vehicle. The control algorithm is designed to overcome the faults arising from the slippage and to keep the vehicle at the desired speed and direction intended by the driver.

Another application of this control algorithm is autonomous vehicles in a platoon system, where the following vehicles should stay at the same speed, acceleration, and direction with the lead vehicle. Preventing the slippage of the wheels of the both the leading and the following vehicle can stop any error at the speed acceleration and direction, and as a consequence any possible collusion.

This paper is organized as follows: The driver assistance systems are introduced and the new concept, adaptive vehicle skid control, is explained in Section 1. System structure of an electrical vehicle is studied in Section 2 and dynamic equations of the system are formulated. In Section 3 an adaptive control approach is used to compensate the uncertainties arising from the road conditions. Section 3.1 explains the operation of the system and in Section 3.2 the problem, changing road friction coefficient, is modeled. In Section 3.3 adaptive control schemes are developed for the unknown and known road condition cases and with Lyapunov stability analyses, the boundedness of the closed-loop signals are proved. Simulation results show the effectiveness of the control algorithm in Section 4. Conclusions and future work for this research are given in Section 5.

2. System structure and dynamics

In order to demonstrate the adaptive controller design for the wheel slip/skid problem, an electrical vehicle is designed, which is shown in Fig. 1. The back wheels of the vehicle have in-wheel electrical motors and the speed of the back wheels can be controlled separately. The front wheels are used for the purpose of steering only and are accompanied by steer by wire system.

For low speed applications, kinematic steering (a.k.a. Ackermann steering) is used to model the motion of the vehicle where the sideslip angles are small so that, the wheels are assumed to be pure rolling. A single-track model (a.k.a. bicycle model) is used to simplify the analysis. The wheels on an axle are represented by a single wheel with the double of cornering stiffness.

In this new study, dynamic steering is used, considering the sideslip angles are big enough to create cornering forces. A single-tack model is not applicable since the back wheels are controlled separately and the cornering forces effecting each front and back wheel can be different because of the possible different road conditions acting on each wheel.

When the model shown in Fig. 2 is considered, the following symbols are utilized as: V is the velocity vector; u is the longitudinal velocity; v is the lateral velocity; β is the sideslip angle; r is the yaw rate; CM is the center of mass; l_f and l_r are the distances between the CM location and the front and the back axles respectively; α_r is the back wheel slip angle; l_t is the wheel tread; F_{dl} is the driving force applied by the left back wheel; F_{dr} is the driving force applied by the right back wheel; F_{bl} is the lateral force at the left back wheel; F_{br} is the lateral force at the right back wheel; F_{fl} is the lateral force at the left front wheel; F_{fr} is the lateral force at the right front wheel; α_{fl} is the left front wheel slip angle; δ_l is the left front wheel steering angle; α_{fr} is the right front wheel slip angle and δ_r is the right front wheel steering angle.

Moreover, the vehicle is assumed to be a rigid body moving on a flat surface and the vehicle has back wheel drive and the front wheels are free rolling. It is also assumed that air resistance, load transfer between the axles,

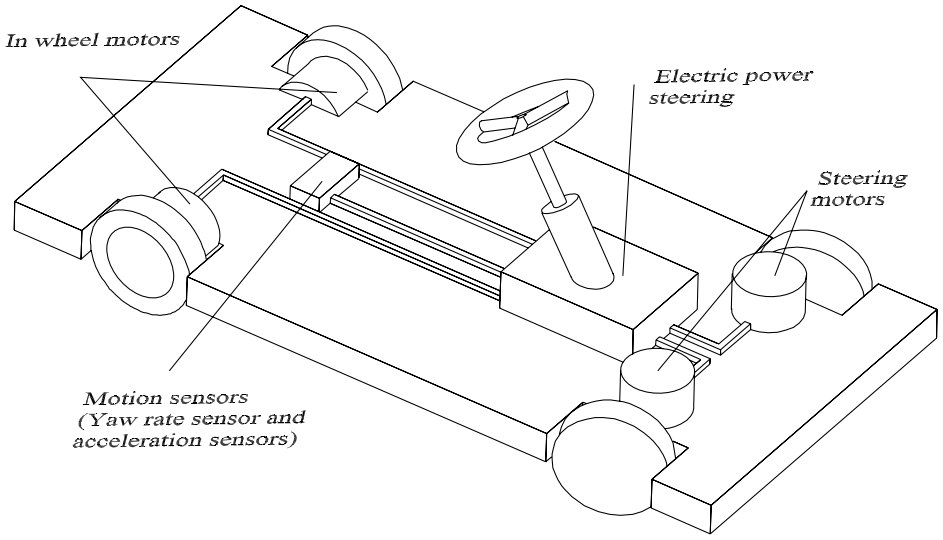

Fig. 1. Prototype electrical vehicle.

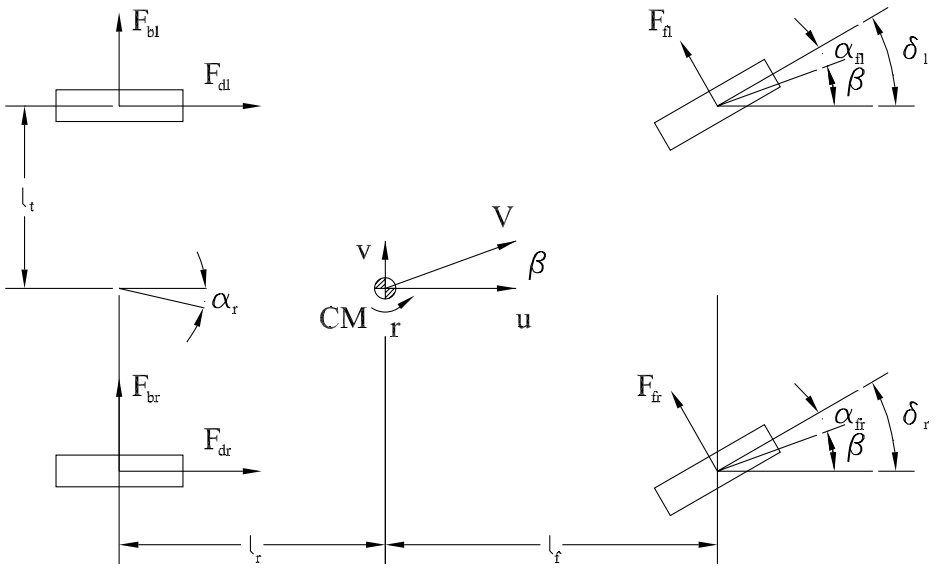

Fig. 2. Dynamical steering of the vehicle.

suspension system dynamics, caster effect and tire dynamics are not included in the dynamics of the vehicle. Interested readers can find more detailed analysis of the vehicle dynamics in [8], since this research is more focused on the design of an adaptive controller, these simplified dynamic equations will be used. With these assumptions, dynamic equations of the system are formulated as

$$m(\dot{u}-rv)=F_{\mathrm{dl}}+F_{\mathrm{dr}}-F_{\mathrm{fl}}\sin(\delta_{\mathrm{l}})-F_{\mathrm{fr}}\sin(\delta_{\mathrm{r}}) \tag{2.1}$$

$$m(\dot{v}+ru)=F_{\mathrm{bl}}+F_{\mathrm{br}}+F_{\mathrm{fl}}\cos(\delta_{\mathrm{l}})+F_{\mathrm{fr}}\cos(\delta_{\mathrm{r}}) \tag{2.2}$$

$$J\dot{r}=l_{\mathrm{f}}(F_{\mathrm{fl}}\sin(\delta_{\mathrm{l}})+F_{\mathrm{fr}}\sin(\delta_{\mathrm{r}}))-l_{\mathrm{r}}(F_{\mathrm{bl}}+F_{\mathrm{br}})+l_{\mathrm{t}}(F_{\mathrm{dr}}-F_{\mathrm{dl}}) \tag{2.3}$$

where m is the vehicle mass and J is the moment of inertia about the vehicle mass center. The first and second equations show the longitudinal and lateral dynamics respectively, where the third equation formulates the yaw motion dynamics. Since the roll and pitch motions are slower than yaw motion [23], they are not included into the dynamic equations.

From the drive wheel dynamics, the driving forces, F_{dl} and F_{dr}, are formulated as

$$F_{\mathrm{d}j}=\begin{cases}\dfrac{\tau_j}{R} & \text{if } \dfrac{\tau_j}{R}\leqslant\dfrac{W_j}{\mu_{\mathrm{b}j}(\sigma)}\\[2ex] \dfrac{W_j}{\mu_{\mathrm{b}j}(\sigma)} & \text{if } \dfrac{\tau_j}{R}>\dfrac{W_j}{\mu_{\mathrm{b}j}(\sigma)}\end{cases} \tag{2.4}$$

where b indicates the back axle, j indicates the wheel, left or right, τ_j is the driving torque applied to the wheel and R is the wheel radius, W_j is the vehicle weight on the wheel $\mu_{\mathrm{b}j}(\sigma)$ is the road surface friction coefficient which is a function of σ wheel slip ratio.

The maximum driving force can be applied to the wheel is formulated as $\frac{W_j}{\mu_{\mathrm{b}j}(\sigma)}$ and if the applied driving force value

$\frac{\tau_j}{R}$ is bigger than the maximum applicable force, the driving force will be equal to the maximum value.

The lateral force effecting each wheel is formulated as the function of the cornering stiffness C_{ij} of the wheel and sideslip angle α_{ij} as

$$F_{ij} = -C_{ij}\alpha_{ij} \tag{2.5}$$

where i indicates the axle: $i = f$ for "front" or $i = b$ for "back", j indicates the wheel: $j = l$ for "left" or $j = r$ for "right".

Cornering stiffness C_{ij} is a function of the road surface friction coefficient and formulated as

$$C_{ij} = C\mu_{ij} \tag{2.6}$$

where C is the cornering coefficient of the tire and μ_{ij} is the friction coefficient effecting the jth wheel at the ith axle.

Sideslip angle α_{ij} is formulated as

$$\alpha_{ij} = \arctan\left(\frac{v + rl_i}{u - rl_t}\right) - \delta_{ij} \tag{2.7}$$

This study assumes equal slip angles on the left and right wheels and only the front wheels are steered. For the simplification of the system steering angles at the front right and left wheels, δ_{fr} and δ_{fl}, are assumed to be the same steering angle $\delta = \delta_{fr} = \delta_{fl}$. Linear tire model is used and the cornering stiffness coefficient C is assumed to be the same for each tire. It should also be noted that the sideslip occurs only when the longitudinal motion exists, ensuring that cornering forces are finite. Under these assumptions, the cornering forces are formulated as

$$F_{bl} = -C\mu_{bl}\arctan\left(\frac{v + rl_r}{u - rl_t}\right) \tag{2.8}$$

$$F_{br} = -C\mu_{br}\arctan\left(\frac{v + rl_r}{u - rl_t}\right) \tag{2.9}$$

$$F_{fl} = -C\mu_{fl}\left(\arctan\left(\frac{v + rl_f}{u - rl_t}\right) - \delta\right) \tag{2.10}$$

$$F_{fr} = -C\mu_{fr}\left(\arctan\left(\frac{v + rl_f}{u - rl_t}\right) - \delta\right) \tag{2.11}$$

Substituting Eqs. (2.8)–(2.11) into (2.1)–(2.3), the dynamic equations of the system are found as

$$\begin{aligned} m\dot{u} = {} & mrv + \frac{\tau_r}{R} + \frac{\tau_l}{R} \\ & + C\sin(\delta)\left(\arctan\left(\frac{v + rl_f}{u - rl_t}\right) - \delta\right)(\mu_{fl} + \mu_{fr}) \end{aligned} \tag{2.12}$$

$$\begin{aligned} m\dot{v} = {} & -mru - C\arctan\left(\frac{v + rl_r}{u - rl_t}\right)(\mu_{bl} + \mu_{br}) \\ & - C\cos(\delta)\left(\arctan\left(\frac{v + rl_f}{u - rl_t}\right) - \delta\right)(\mu_{fl} + \mu_{fr}) \end{aligned} \tag{2.13}$$

$$\begin{aligned} J\dot{r} = {} & -l_f C\sin(\delta)\left(\arctan\left(\frac{v + rl_f}{u - rl_t}\right) - \delta\right)(\mu_{fl} + \mu_{fr}) \\ & + l_r C\arctan\left(\frac{v + rl_r}{u - rl_t}\right)(\mu_{bl} + \mu_{br}) + \frac{l_t}{R}(\tau_r - \tau_l) \end{aligned} \tag{2.14}$$

which can be rewritten as

$$D\ddot{q} = f(\dot{q}, \mu_{ij}) + g(\dot{q}, \tau, \mu_{ij}) \tag{2.15}$$

where μ_{ij} is the friction coefficient effecting the jth wheel at the ith axle, i indicates the axle, front or back, j indicates the wheel, left or right, the sate vector $\dot{q}$ and the control input vector τ are formulated as respectively, $\dot{q} = [u, v, r]^T$ and $\tau = [\delta, \tau_r, \tau_l]$. The positive-definite mass matrix D, the term containing the unaffected dynamics from the control input $f(\dot{q}, \mu_{ij})$ and the term contains the controllable dynamics $g(\dot{q}, \tau, \mu_{ij})$ are formulated as respectively

$$D = \begin{bmatrix} m & 0 & 0 \\ 0 & m & 0 \\ 0 & 0 & J \end{bmatrix} \tag{2.16}$$

$$f(\dot{q}, \mu_{ij}) = \begin{bmatrix} mrv \\ -mru - C\arctan\left(\frac{v + rl_r}{u - rl_t}\right)(\mu_{bl} + \mu_{br}) \\ l_r C\arctan\left(\frac{v + rl_r}{u - rl_t}\right)(\mu_{bl} + \mu_{br}) \end{bmatrix} \tag{2.17}$$

$$\begin{aligned} & g(\dot{q}, \tau, \mu_{ij}) \\ & = \begin{bmatrix} C\sin(\delta)\left(\arctan\left(\frac{v + rl_f}{u - rl_t}\right) - \delta\right)(\mu_{fl} + \mu_{fr}) + \frac{\tau_r}{R} + \frac{\tau_l}{R} \\ -C\cos(\delta)\left(\arctan\left(\frac{v + rl_f}{u - rl_t}\right) - \delta\right)(\mu_{fl} + \mu_{fr}) \\ -l_f C\sin(\delta)\left(\arctan\left(\frac{v + rl_f}{u - rl_t}\right) - \delta\right)(\mu_{fl} + \mu_{fr}) + \frac{l_t}{R}(\tau_r - \tau_l) \end{bmatrix} \end{aligned} \tag{2.18}$$

3. Adaptive wheel skid control

3.1. System operation

Driver assistance systems can be categorized into three different groups by their application area [4]. Longitudinal control involves keeping the vehicle at a designated distance from the prior vehicle maintaining a relatively constant speed. This is accomplished by using cruise control and adaptive cruise control systems, where radar is added to a standard cruise control to measure the distance and the speed of the prior vehicle to adjust the following distance and the speed of the vehicle. Anti-lock brake systems (ABS) and traction control systems (TCS) can be categorized in the longitudinal vehicle control systems, where these systems are designed to prevent skidding in the longitudinal dynamics.

Lateral control of the vehicle is achieved by look-down and look-ahead reference systems and accomplishes the low speed steering of the vehicle. Lane keeping, lane changing, turning, avoiding obstacles, steering over correction because of a flat tire and lane departure problems are solved by lateral control algorithms.

The direct yaw moment control system, a combination of longitudinal and lateral control systems, is used to control the vehicle at high speed steering. This system stabilizes

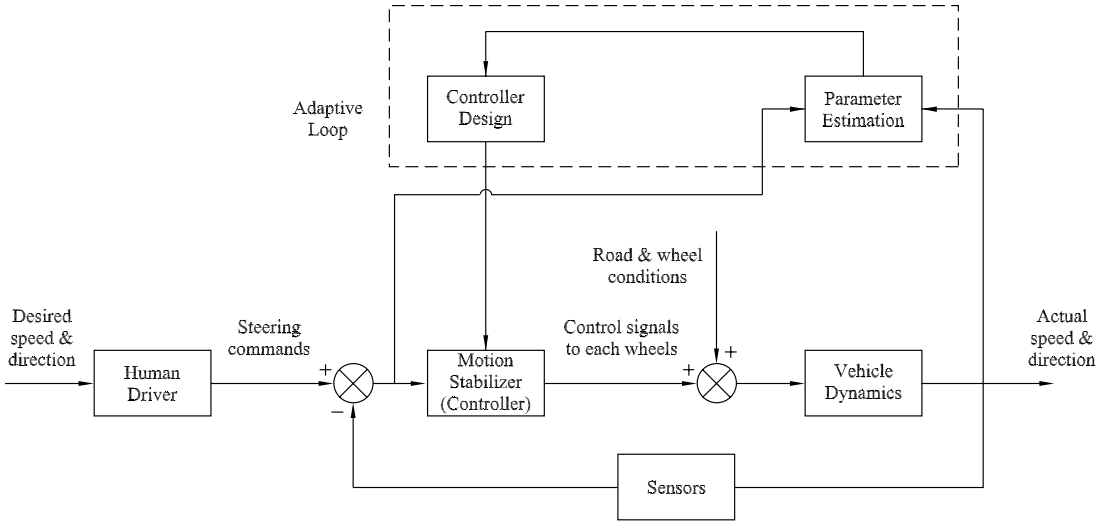

Fig. 3. Block diagram of the proposed driver assistance system.

the motion of the vehicle by braking the slipping wheel and bringing it to a skid range that it can start applying driving force again [21]. In the current direct yaw moment system technology, the skidding wheel is detected and the power applied to this wheel is reduced, until the traction is regained. However, when the total vehicle dynamic is considered, after the skidding occurs, in order to regain control of the vehicle, the total speed of the vehicle is reduced, which can be a problem in traffic, because accidents occur when any vehicle's speed suddenly decreases.

In the proposed system, the speed and the direction of the vehicle are designed to be maintained as desired by the driver. A motion stabilizer system whose block diagram is shown in Fig. 3 is proposed. The operation of the motion stabilizer is as follows: The speed and the direction of the vehicle are determined by the driver. In case of a wheel slippage, an adaptive control algorithm keeps the speed of the vehicle as desired by applying more power to the drive wheels where the additional driving force at the non-skidding wheel will compensate for the loss of the driving force at the skidding wheel, and the controller also arranges the direction of the vehicle by changing the steering angle of the steering wheels.

3.2. Problem formulation

While a ground vehicle is travelling on the road, the forces acting on the vehicle are the functions of the road friction coefficient and these driving forces are formulated as

$$F_{\mathrm{d}j} = \begin{cases} \dfrac{\tau_j}{R} & \text{if } \dfrac{\tau_j}{R} \leqslant \dfrac{W_j}{\mu_{\mathrm{b}j}(\sigma)} \\ \dfrac{W_j}{\mu_{\mathrm{b}j}(\sigma)} & \text{if } \dfrac{\tau_j}{R} > \dfrac{W_j}{\mu_{\mathrm{b}j}(\sigma)} \end{cases} \tag{3.1}$$

where b indicates the back axle, j indicates the wheel, left or right, τ_j is the driving torque applied to the wheel and R is the wheel radius, W_j is the vehicle weight on the wheel $\mu_{\mathrm{b}j}(\sigma)$ is the road surface friction coefficient which is a function of σ wheel slip ratio. Lateral forces are formulated as

$$F_{ij} = -C\mu_{ij}\alpha_{ij} \tag{3.2}$$

where C is the cornering coefficient of the tire and μ_{ij} is the friction coefficient, α_{ij} is the sideslip angle effecting the jth wheel at the ith axle.

On different road surfaces, the road friction coefficients, which are functions of slip ratio, vary and for an example tire are shown in Fig. 4. The road friction coefficient is found experimentally, but also can be approximated by an analytical expression. A general expression in the range of $-1 < \sigma < 1$ is

$$\mu = a(1 - \mathrm{e}^{-b\sigma}) + c\sigma^2 - d\sigma \tag{3.3}$$

where the coefficients a, b, c and d are obtained from the experimental curves and σ is the slip ratio and is defined as

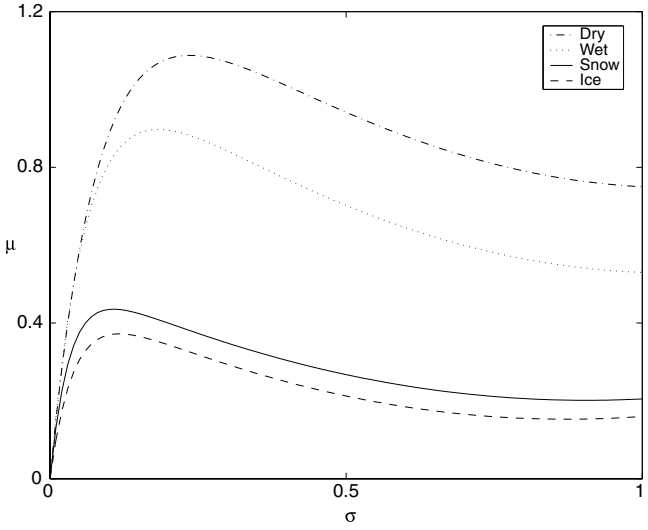

Fig. 4. Tire friction coefficient vs. wheel slip.

$$\sigma = \frac{R\omega - v}{R\omega} \tag{3.4}$$

where R is the wheel radius, ω is the angular speed of the wheel and v is the linear speed of the wheel center. The ABS system will not allow the wheel to get locked, this means ω will not be zero and σ, slip ratio, is always defined.

At different surfaces (i.e., dry asphalt, wet asphalt or ice) the a, b, c, d coefficients will differ. The uncertainty in the road friction confection is expressed as

$$\mu_{ij} = \mu_{ij1}\lambda_{ij1}(t) + \mu_{ij2}\lambda_{ij2}(t) + \cdots + \mu_{ijk}\lambda_{ijk}(t) \tag{3.5}$$

where μ_{ij} is the actual road friction coefficient at the ith axle jth wheel, μ_{ijp}, $p = 1,\ldots,k$, are road friction coefficients for different surfaces, which last a certain period of time, and $\lambda_{ijp}(t)$ are time functions indicating which values of μ_{ijp} are taken by μ_{ij} at a given time. μ_{ij} is a function of time showing the ith axle jth wheel road friction coefficient.

$$\lambda_{ijp} = \begin{cases} 1 & \text{if } \mu_{ij} = \mu_{ijp} \\ 0 & \text{otherwise} \end{cases} \tag{3.6}$$

Function $\lambda_{ijp}(t)$ indicates only one value can be active at any time, that is $\lambda_{ijm}(t)\lambda_{ijn}(t) = 0$, for $m \neq n$, and $\lambda_{ij1} + \lambda_{ij2} + \cdots + \lambda_{ijk} = 1$.

The following two cases are possible for $\lambda_{ijp}(t)$

(i) The road condition information is not available, that is, $\lambda_{ijp}(t)$ are unknown;
(ii) The road condition is measured, that is, $\lambda_{ijp}(t)$ are known.

While the real values of μ_{ijp} are not known, these bounds can be found experimentally. When the road condition is measured, $\lambda_{ijp}(t)$ are known.

During the field test the friction coefficients will require tuning, because there is no exact friction coefficient value for an icy road. However, the adaptive control algorithm ensures that with the parameter update laws, arbitrarily guessed unknown parameter values are converged to the values that makes the system error converge to zero, where the system is stable.

The controller objective is to design a feedback control law τ for the system (2.15) to ensure that all closed-loop system signals and parameter estimates are bounded, and that the system output $q(t)$ asymptotically tracks a given reference output $q_d(t)$. In other words, the controller objective is to keep the speed and the direction of the vehicle as desired by the driver, despite the uncertainties arising from the road conditions.

3.3. Adaptive controller design

Because of computing difficulties there were some assumptions made in the previous section during the formulation of the mathematical model of the system. There are also measuring difficulties in the system, which causes more assumptions, such as the mass and the inertia of the vehicle, since these values would change with the number of passengers. These assumptions cause uncertainties and in order to compensate for these uncertainties in the system, adaptive control methods are used. The adaptive control system uses the knowledge from plant dynamics and updates the control parameters on-line to eliminate the tracking error.

3.3.1. Design with unknown road condition

When there is no information available about the road condition, the adaptive control scheme can be derived in the following procedure. The term, including the control inputs in the dynamical equations of the system, $g(\dot{q}, \tau, \mu_{ij})$ in (2.18), is expressed as

$$g(\dot{q}, \tau, \mu_{ij}) = K_\tau \tau \tag{3.7}$$

where $\tau = [\delta, \tau_r, \tau_l]^T$ and

$$K_\tau = \begin{bmatrix} \dfrac{C\sin(\delta)(A-\delta)(\mu_{fl}+\mu_{fr})}{\delta} & \dfrac{1}{R} & \dfrac{1}{R} \\ \dfrac{-C\cos(\delta)(A-\delta)(\mu_{fl}+\mu_{fr})}{\delta} & 0 & 0 \\ \dfrac{-l_f C\sin(\delta)(A-\delta)(\mu_{fl}+\mu_{fr})}{\delta} & \dfrac{l_t}{R} & -\dfrac{l_t}{R} \end{bmatrix} \in R^{3\times 3} \tag{3.8}$$

with $A = \arctan(\frac{v+rl_f}{u-rl_t})$.

Let $\hat{K}_\tau$ be the estimate of K_τ and choose the control law as

$$\tau = \hat{K}_\tau^{-1}\tau_d \tag{3.9}$$

where τ_d is a feedback control law designed based on the ideal system

$$D\ddot{q} = f(\dot{q}, \mu_{ij}) + \tau_d \tag{3.10}$$

The existence of $\hat{K}_\tau^{-1}$ is to be ensured by a projection algorithm in the adaptive law for updating the estimate $\hat{K}_\tau(t)$. From (2.15), (3.7) and (3.9), the closed-loop dynamic equation is

$$D\ddot{q} = f(\dot{q}, \mu_{ij}) + (K_\tau - \hat{K}_\tau)\tau + \tau_d \tag{3.11}$$

The ideal matching parameter for $\hat{K}_\tau(t)$ is K_τ.

To design an adaptive control scheme to handle parameter uncertainties, for $\dot{q} = [u, v, r]^T$ and $\dot{q}_d = [u_d, v_d, r_d]^T$, the tracking error e and the filtered tracking errors $s, \dot{s}$ are defined as

$$e = q - q_d, \quad \dot{e} = \dot{q} - \dot{q}_d \tag{3.12}$$

$$s = \dot{e} + \eta e, \quad \dot{s} = \ddot{e} + \eta\dot{e} \tag{3.13}$$

where $\eta \in R^{3\times 3} > 0$ is a diagonal gain matrix.

At first the ideal system is expressed as $D\ddot{q} = f(\dot{q}, \mu_{ij}) + \tau_d$ as $D\dot{s} = -Y(\dot{q}, \ddot{q}, h)\theta + \tau_d$, where

$$Y(\dot{q}, \ddot{q}, h)\theta = Dh - f(\dot{q}, \mu_{ij}), h = \ddot{q}_d - \eta\dot{e} \tag{3.14}$$

where $Y(\dot{q}, \ddot{q}, h) \in R^{3\times 4}$ is a known matrix function, $\theta(m, \mu_{ij}, J) \in R^{4\times 1}$ is an unknown parameter vector and are formulated as

$$Y(\dot{q},\ddot{q},h)=\begin{bmatrix} h_1-rv & 0 & 0 & 0 \\ h_2+ru & 0 & CA & CA \\ 0 & h_3 & -l_rCA & -l_rCA \end{bmatrix} \tag{3.15}$$

$$\theta=[m,J,\mu_{\mathrm{bl}},\mu_{\mathrm{br}}]^{\mathrm{T}}. \tag{3.16}$$

The actual system (3.11) is expressed as

$$D\dot{s}=-Y\theta-(\hat{K}_\tau-K_\tau)\tau+\tau_{\mathrm{d}} \tag{3.17}$$

for which $K_\tau\tau$ can be further expressed as

$$K_\tau\tau=Y_\tau\theta_\tau \tag{3.18}$$

where

$$\theta_\tau=\left[\mu_{\mathrm{fr}},\mu_{\mathrm{fl}},\frac{1}{R}\right]^{\mathrm{T}} \tag{3.19}$$

is the parameter vector, and

$$Y_\tau=\begin{bmatrix} C\sin(\delta)(A-\delta) & C\sin(\delta)(A-\delta) & (\tau_{\mathrm{r}}+\tau_{\mathrm{l}}) \\ -C\cos(\delta)(A-\delta) & -C\cos(\delta)(A-\delta) & 0 \\ -l_{\mathrm{f}}C\sin(\delta)(A-\delta) & -l_{\mathrm{f}}C\sin(\delta)(A-\delta) & l_{\mathrm{t}}(\tau_{\mathrm{r}}-\tau_{\mathrm{l}}) \end{bmatrix} \tag{3.20}$$

is the known matrix function.

Let $\hat{\theta}_\tau$ be the estimate of θ_τ. Then, the dynamical system (3.17) becomes

$$D\dot{s}=-Y\theta-Y_\tau(\hat{\theta}_\tau-\theta_\tau)+\tau_{\mathrm{d}} \tag{3.21}$$

For this system, the control law is designed as

$$\tau_{\mathrm{d}}=Y\hat{\theta}-K_Ds \tag{3.22}$$

where $K_D=K_D^{\mathrm{T}}>0$, $K_D\in R^{3\times3}$ is a gain matrix, $\hat{\theta}$ is the estimate of θ, updated from an adaptive law. This control law could also be used for the ideal system $D\dot{s}=-Y\theta+\tau_{\mathrm{d}}$.

With the control law (3.22), the closed-loop system is

$$D\dot{s}=Y(\hat{\theta}-\theta)-Y_\tau(\hat{\theta}_\tau-\theta_\tau)-K_Ds \tag{3.23}$$

A Lyapunov-like positive-definite scalar function is chosen as

$$V_1(t)=\frac{1}{2}s^{\mathrm{T}}Ds+\frac{1}{2}\tilde{\theta}^{\mathrm{T}}\Gamma_1^{-1}\tilde{\theta}+\frac{1}{2}\tilde{\theta}_\tau^{\mathrm{T}}\Gamma_2^{-1}\tilde{\theta}_\tau \tag{3.24}$$

where $\tilde{\theta}=\hat{\theta}-\theta$, $\tilde{\theta}_\tau=\hat{\theta}_\tau-\theta_\tau$, $\Gamma_1=\Gamma_1^{\mathrm{T}}>0$ and $\Gamma_2=\Gamma_2^{\mathrm{T}}>0$.

For the time t in each interval when the values of θ and θ_τ do not change, differentiating (3.24) with respect to the time t and using (3.23) yields

$$\dot{V}_1=\tilde{\theta}^{\mathrm{T}}(\Gamma_1^{-1}\dot{\tilde{\theta}}+Y^{\mathrm{T}}s)+\tilde{\theta}_\tau^{\mathrm{T}}(\Gamma_2^{-1}\dot{\tilde{\theta}}_\tau-Y_\tau^{\mathrm{T}}s)-s^{\mathrm{T}}K_Ds \tag{3.25}$$

Choose the adaptive parameter update laws for $\dot{\hat{\theta}}$ and $\dot{\hat{\theta}}_\tau$ as

$$\dot{\hat{\theta}}=\dot{\tilde{\theta}}=-\Gamma_1Y^{\mathrm{T}}s \tag{3.26}$$

$$\dot{\hat{\theta}}_\tau=\dot{\tilde{\theta}}_\tau=\Gamma_2Y_\tau^{\mathrm{T}}s \tag{3.27}$$

which are defined for all $t\geqslant0$. Then, the derivative of the Lyapunov-like function is found as

$$\dot{V}_1=-s^{\mathrm{T}}(t)K_Ds(t)\leqslant0 \tag{3.28}$$

for t in each interval when the values of θ and θ_τ do not change.

The Lyapunov-like function $V_1(t)$ is positive-definite and $\dot{V}_1$ is negative semi-definite. Stability in the sense of Lyapunov has been shown in that the position tracking and velocity tracking errors are both bounded. When a slip occurs at any of the wheels of the vehicle, a bounded jump occurs in the Lyapunov-like function $V_1(t)$, where its derivative $\dot{V}_1$ is undefined. The stability of the system is valid for every each time interval between the occurrence of each jump. Due to possible persistent uncertain jumps, the tracking error may not converge to zero. However, if there are only a finite number of jumps, the developed adaptive control scheme ensures that the tracking error converges to zero asymptotically. For the case when the parameter jumps are persistent, that is, the vehicle keeps entering a surface at one time and another surface at another time, practical tracking is achievable if the time interval of switching surface is large enough. In this case, to ensure asymptotic tracking, a modified adaptive control scheme can be developed, using certain additional system information (see the known road condition case).

In order to ensure that $\hat{K}_\tau(t)$ has a bounded inverse $\hat{K}_\tau^{-1}(t)$, a projection algorithm is used in the design of the adaptive update law. The term $\hat{K}_\tau\tau$ is expressed as

$$\hat{K}_\tau\tau=Y_\tau(\delta,\tau_{\mathrm{r}},\tau_{\mathrm{l}})\hat{\theta}_\tau \tag{3.29}$$

where $\hat{\theta}_\tau$ is the estimate of the parameter vector and $Y_\tau(\delta,\tau_{\mathrm{r}},\tau_{\mathrm{l}})$ is the known signal vector.

The adaptive update law for $\hat{\theta}_\tau$ is given in Eq. (3.27) as

$$\dot{\hat{\theta}}_\tau=\dot{\tilde{\theta}}_\tau=\Gamma_2Y_\tau^{\mathrm{T}}s \tag{3.30}$$

and by applying a projection algorithm defined as

$$\dot{\hat{\theta}}_\tau=G(t) \tag{3.31}$$

$$G(t)=(G_1(t),\ldots,G_4(t))^{\mathrm{T}}\in R^4 \tag{3.32}$$

where the size of $G(t)$ is equal to the size of θ_τ which consists of four unknown parameters namely μ_{fr}, μ_{fl}, μ_{br} and μ_{bl}.

$$G_k(t)=\begin{cases} & \text{if } \hat{\theta}_{\tau k}(t)\in(\theta_{\tau k}^a,\theta_{\tau k}^b) \text{ or} \\ F_k(t) & \text{if } \hat{\theta}_{\tau k}(t)=\theta_{\tau k}^a \text{ and } F_k(t)\geqslant0 \text{ or} \\ & \text{if } \hat{\theta}_{\tau k}(t)=\theta_{\tau k}^b \text{ and } F_k(t)\leqslant0 \\ 0 & \text{otherwise} \end{cases} \tag{3.33}$$

where $F(t)$ is defined as $F(t)=(F_1(t),\ldots,F_4(t))^{\mathrm{T}}=\Gamma_2Y_\tau^{\mathrm{T}}s$ and $\theta_{\tau k}\in[\theta_{\tau k}^a,\theta_{\tau k}^b],k=1,\ldots,4$, $\hat{\theta}_{\tau k}$ and $\theta_{\tau k}$ are the kth components of $\hat{\theta}_\tau$ and θ_τ, respectively, $\theta_{\tau k}^a,\theta_{\tau k}^b,k=1,\ldots,4$, are known such that for any $\hat{\theta}_{\tau k}\in[\theta_{\tau k}^a,\theta_{\tau k}^b]$, where $\theta_{\tau k}^a$ is the upper limit of μ_{ij}, which is μ_{dry} and $\theta_{\tau k}^b$ is the lower limit of μ_{ij}, which is μ_{ice}, $k=1,\ldots,4$, the resulting $\hat{K}_\tau(t)$ is invertible, that is, $\hat{K}_\tau^{-1}(t)$ is bounded, and n is the degree of the differential equations representing the dynamics of the system, which is two in this study. It can be verified that the

desired property (3.28) still holds, and in addition, it is ensured that $\hat{\theta}_{\tau k} \in [\theta^a_{\tau k}, \theta^b_{\tau k}], k = 1, \ldots, 4$, so that $\hat{K}_\tau^{-1}(t)$ is bounded.

3.3.2. Design with known road condition

It is possible to measure the road condition by using a millimeter radiometer, a radar sensor [24–26], in the sense it is known whether the vehicle is on a dry surface or on an icy surface, but the road friction coefficients are assumed to be unknown, that is, $\lambda_{ijp}(t)$ are known, but μ_{ijp} are unknown.

Using (3.5) and (3.6), we express $g(\dot{q}, \tau, \mu_{ij})$ in (2.15) as

$$g(\dot{q}, \tau, \mu_{ij}) = (K\tau_1\lambda_{ij1} + K\tau_2\lambda_{ij2} + \cdots + K\tau_k\lambda_{ijk})\tau \tag{3.34}$$

where

$$K\tau_p = \begin{bmatrix} \dfrac{C\sin(\delta)(A-\delta)(\mu_{flp}+\mu_{frp})}{\delta} & \dfrac{1}{R} & \dfrac{1}{R} \\ \dfrac{C\cos(\delta)(A-\delta)(\mu_{flp}+\mu_{frp})}{\delta} & 0 & 0 \\ \dfrac{-l_f C\sin(\delta)(A-\delta)(\mu_{flp}+\mu_{frp})}{\delta} & \dfrac{l_t}{R} & -\dfrac{l_t}{R} \end{bmatrix}$$
$$p = 1, 2, \ldots, k \tag{3.35}$$

where $A = \arctan(\frac{v+rl_f}{u-rl_t})$.

Let $\hat{K}_{\tau p}$ be the estimate of $K_{\tau p}$, $p = 1,2,\ldots,k$, and choose the control law as

$$\tau = (\hat{K}_{\tau 1}^{-1}\lambda_{ij1}(t) + \cdots + \hat{K}_{\tau p}^{-1}\lambda_{ijp}(t))\tau_d \tag{3.36}$$

Then Eq. (3.11) becomes

$$D\ddot{q} = f(\dot{q}, \mu_{ij}) + (K_{\tau 1} - \hat{K}_{\tau 1}\lambda_{ij1}(t) + \cdots + K_{\tau p} - \hat{K}_{\tau p}\lambda_{ijp}(t))\tau + \tau_d. \tag{3.37}$$

Considering that $\tau_p = \lambda_{ijp}\tau$ and inserting this equation into the previous equation results as

$$D\ddot{q} = f(\dot{q}, \mu_{ij}) + (K_{\tau 1} - \hat{K}_{\tau 1})\tau_1 + \cdots + (K_{\tau p} - \hat{K}_{\tau p})\tau_k + \tau_d. \tag{3.38}$$

$f(\dot{q}, \mu_{ij})$ formulated as

$$f(\dot{q}, \mu_{ij}) = -Y(\dot{q}, \ddot{q}, h)(\theta_1\lambda_{ij1} + \theta_2\lambda_{ij2} + \cdots + \theta_k\lambda_{ijk}) \tag{3.39}$$

By including $Y_p = Y\lambda_{ijp}$ and Eq. (3.39) into Eq. (3.38), the actual system is expressed as

$$D\dot{s} = -(Y_1\theta_1 + Y_2\theta_2 + \cdots + Y_k\theta_k) - (K_{\tau 1} - \hat{K}_{\tau 1})\tau_1 - (K_{\tau 2} - \hat{K}_{\tau 2})\tau_2 - \cdots - (K_{\tau k} - \hat{K}_{\tau k})\tau_k + \tau_d \tag{3.40}$$

Considering that

$$K_\tau\tau = Y_{\tau 1}(\delta, \tau_r, \tau_l)\theta_{\tau 1} + Y_{\tau 2}(\delta, \tau_r, \tau_l)\theta_{\tau 2} + \cdots + Y_{\tau k}(\delta, \tau_r, \tau_l)\theta_{\tau k} \tag{3.41}$$

$$\hat{K}_\tau\tau = Y_{\tau 1}(\delta, \tau_r, \tau_l)\hat{\theta}_{\tau 1} + Y_{\tau 2}(\delta, \tau_r, \tau_l)\hat{\theta}_{\tau 2} + \cdots + Y_{\tau k}(\delta, \tau_r, \tau_l)\hat{\theta}_{\tau k} \tag{3.42}$$

and by choosing the control law as

$$\tau_d = Y_1\hat{\theta}_1 + Y_2\hat{\theta}_2 + \cdots + Y_k\hat{\theta}_k - K_D s \tag{3.43}$$

the closed-loop system becomes

$$D\dot{s} = Y_1(\hat{\theta}_1 - \theta_1) + Y_2(\hat{\theta}_2 - \theta_2) + \cdots + Y_k(\hat{\theta}_k - \theta_k) - Y_{\tau 1}(\hat{\theta}_{\tau 1} - \theta_{\tau 1}) - Y_{\tau 2}(\hat{\theta}_{\tau 2} - \theta_{\tau 2}) - \cdots - Y_{\tau k}(\hat{\theta}_{\tau k} - \theta_{\tau k}) - K_D s \tag{3.44}$$

A Lyapunov-like positive-definite scalar function is chosen as

$$V_2 = \frac{1}{2}s^T D s + \frac{1}{2}\sum_{p=1}^{k}\tilde{\theta}_p^T\Gamma_p^{-1}\tilde{\theta}_p + \frac{1}{2}\sum_{p=1}^{k}\tilde{\theta}_{\tau p}^T\Gamma_{\tau 2}^{-1}\tilde{\theta}_{\tau p} \tag{3.45}$$

For the time t in each interval when the values of θ_p and $\theta_{\tau p}$ do not change, differentiating (3.45) with respect to the time t and using (3.44) yields

$$\dot{V}_2 = \sum_{p=1}^{k}\tilde{\theta}_p^T(\Gamma_p^{-1}\dot{\tilde{\theta}}_p + Y_p^T s) + \sum_{p=1}^{k}\tilde{\theta}_{\tau p}^T(\Gamma_{\tau p}^{-1}\dot{\tilde{\theta}}_{\tau p} + Y_{\tau p}^T s) - s^T K_D s \tag{3.46}$$

Choose the adaptive parameter update laws for $\dot{\tilde{\theta}}_p$ and $\dot{\tilde{\theta}}_{\tau p}$ as

$$\dot{\hat{\theta}}_p = \dot{\tilde{\theta}}_p = -\Gamma_p Y_p^T s \tag{3.47}$$

$$\dot{\hat{\theta}}_{\tau p} = \dot{\tilde{\theta}}_{\tau p} = \Gamma_2 Y_{\tau p}^T s, \qquad p = 1, 2, \ldots, k \tag{3.48}$$

which are defined for all $t \geqslant 0$, and the derivative of the Lyapunov-like function is found as

$$\dot{V}_2 = -s^T K_D s(t) \leqslant 0 \tag{3.49}$$

for t in each interval when the values of θ_p and $\theta_{\tau p}$ do not change, the Lyapunov-like function $V_2(t)$ is valid over the time interval for each change in the road friction coefficient for each wheel.

The fact that $\dot{V}_2 = -s^T K_D s \leqslant 0$ implies $s \in L^2 \cap L^\infty$ and θ_p and $\theta_{\tau p} \in L^\infty$ for $p = 1, \ldots, k$. Since $s = \dot{e} + \eta e$, it implies e and $\dot{e} \in L^2 \cap L^\infty$, and also q and $\dot{q} \in L^\infty$. From (3.22) it follows that τ_d and $\dot{s} \in L^\infty$ which results $\ddot{e} \in L^\infty$. By applying the Barbălat Lemma [27] it is concluded that the position tracking error e and velocity tracking error $\dot{e}$ go to zero as t goes to ∞.

In summary, it is proven that with the control law (3.43) and adaptive update laws (3.47) and (3.48), when the road condition is measured, it is guaranteed that all closed-loop signals are bounded and the tracking error $e(t)$ and $\dot{e}(t)$ go to zero as t goes to ∞.

In order to ensure that $\hat{K}_\tau(t)$ has a bounded inverse $\hat{K}_\tau^{-1}(t)$, a projection algorithm is used in the design of the adaptive update law same as before.

4. Simulation results

The vehicle model formulated in Eqs. (2.15)–(2.18) is used in the simulations. Since, this study is more focused

on design of the control algorithm, the assumptions mentioned in Chapter 2 are made. Another assumption made in this research is also the fact that the driver's reaction is not important, since the purpose of this research is to demonstrate the design of the control algorithm. In reality, the driver's reaction will be very important, and should be included in the field test of this algorithm on a model car. This is what we would like to achieve in the future research.

In this simulation study, the vehicle design shown in Fig. 1 is driven on a straight road with a 10 m/s constant

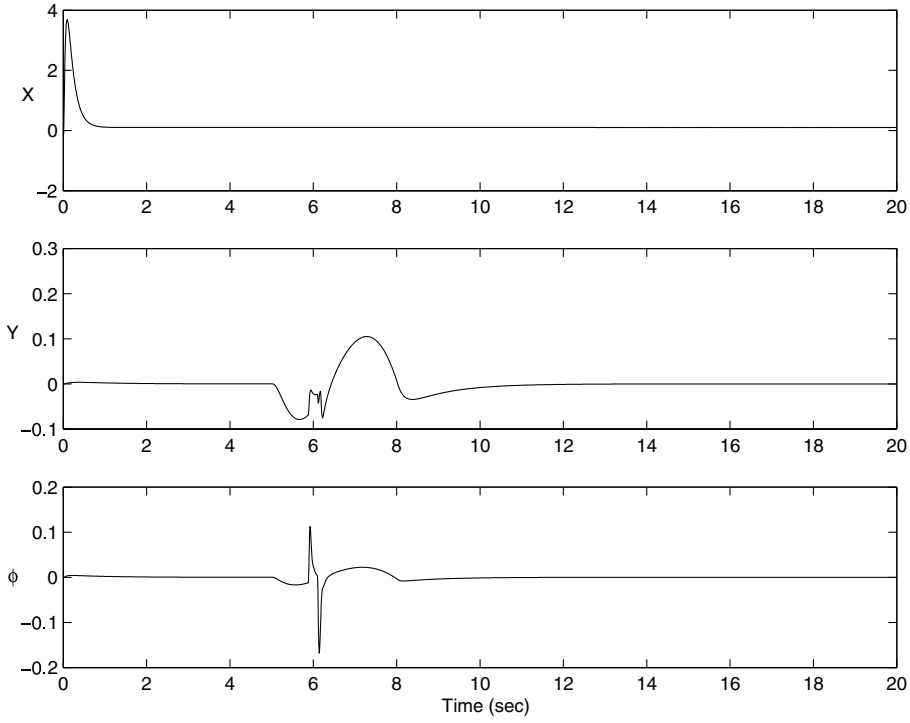

Fig. 5. Position errors.

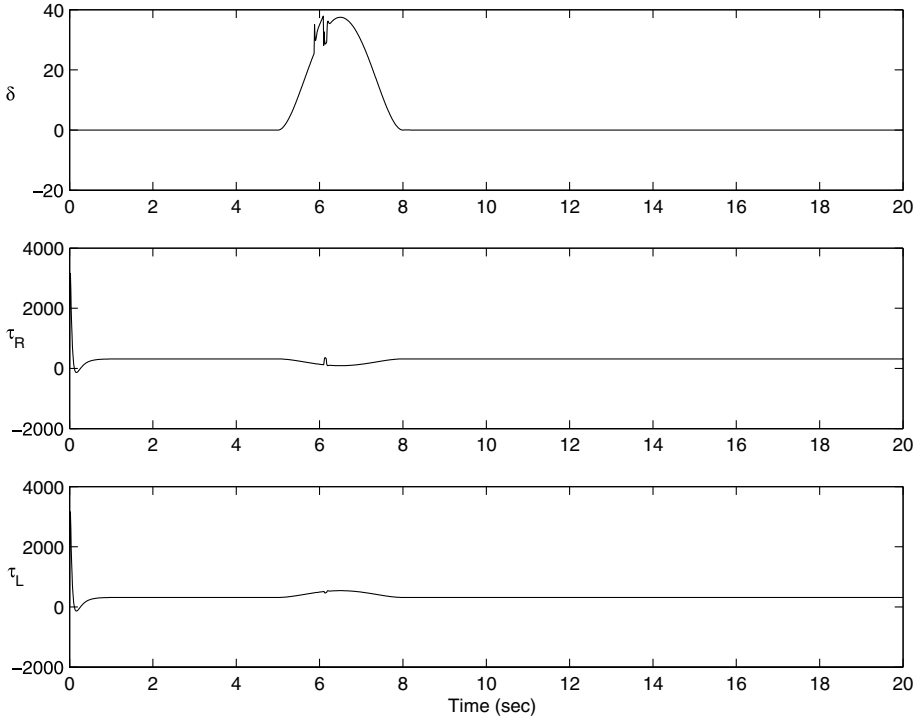

Fig. 6. Control inputs.

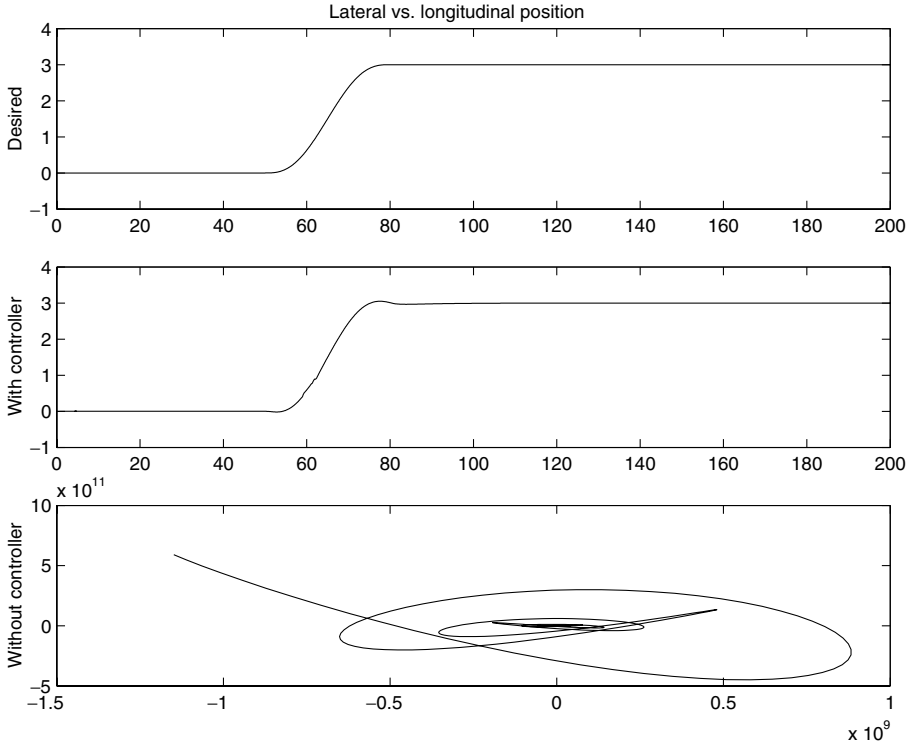

Fig. 7. Effect of the controller.

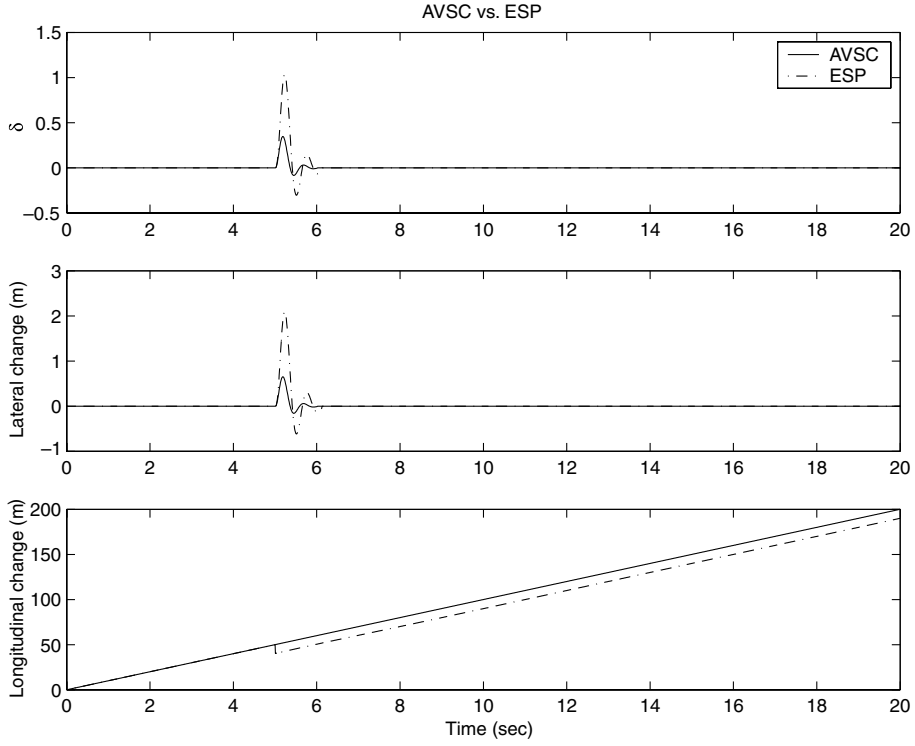

Fig. 8. Comparison of the AVSC system to an ESP system.

speed. At the fifth second the driver realizes the ice on the road and maneuvers the vehicle to the left, but the rear right wheel drives on the ice and the effect of the changing friction coefficient is shown in the following figures. Fig. 5 shows the position errors in the longitudinal, lateral and angular directions. Fig. 6 demonstrates the change in the control inputs because of the changing road conditions. The effect of the known road condition controller is shown

in Fig. 7, where with the controller can achieve the desired performance, but without the controller the system becomes unstable.

Fig. 8. shows the advantages of the proposed control system Adaptive Vehicle Skid Control (AVSC) to an ESP system studied in [28], where the earlier simulation is repeated for both AVSC and ESP systems. The result is the vehicle with an AVSC system continues with the same speed whereas the vehicle with an ESP system cannot keep its intended position in the longitudinal direction.

5. Concluding remarks

In this research, adaptive vehicle skid control concept is developed. Dynamic equations of an electric vehicle are formulated and the effect of the road friction coefficient is studied. When the road condition information is not available, the boundedness of the position and velocity error is proved. In the second part of the research, the performance of the controller is examined when the road condition is measured (but the road friction coefficients are assumed not to be known). Simulation results show the effectiveness of the controller schemes. The effect of a flat tire and roll-over resistance of the vehicle, by selecting the steering angles δ_{fl} and δ_{fr} differently, will also be studied for future research.

References

[1] van der Voort MC. FEST. A new driver support tool that reduces fuel consumption and emissions. Int Conf Adv Driver Assistance Syst 2001:90–3.

[2] Mammar S, Baghdassarian VB. Two-degree-of-freedom formulation of vehicle handling improvement by active steering. Proc Amer Contr Conf 2000;1:105–9.

[3] Fodor M, Yester J, Hrovat D. Active control of vehicle dynamics. Proc Digital Avionics Syst Conf 1998;2:I14/1–8.

[4] Nobe SA, Fei-Yue W. An overview of recent developments in automated lateral and longitudinal vehicle controls. Int Conf Syst, Man, Cyber 2001;5:3447–52.

[5] Johansen TA, Kalkkuhl J, Ludemann J, Petersen I. Hybrid control strategies in ABS. Proc Amer Contr Conf 2001;2:1704–5.

[6] Wong JY. Theory of ground vehicles. New York: John Wiley & Sons; 2001.

[7] Sakai S, Sado H, Hori Y. Motion control in an electric vehicle with four independently driven in-wheel motors. IEEE Trans Mech 1999;4(1):9–16.

[8] Genta G. Motor vehicle dynamics modeling and simulation. Singapore: World Scientific Publishing Co. Pte. Ltd.; 1997.

[9] Drakunov SV, Ashrafi B, Rosiglioni A. Yaw control algorithm via sliding mode control. Proc Amer Contr Conf 2000;1:580–3.

[10] Kaoru S, Yoshiaki S. Application of active yaw control to vehicle dynamics by utilizing driving/breaking force. JSAE Rev 1999;20(2):289–95.

[11] Bevly DM, Gerdes JC, Wilson C, Gengsheng Z. The use of GPS based velocity measurements for improved vehicle state estimation. Proc Amer Contr Conf 2001;4:2538–42.

[12] Tseng HE, Ashrafi B, Madau D, Allen Brown T, Recker D. The development of vehicle stability control at Ford. IEEE Trans Mech 1999;4(3):223–34.

[13] Sado H, Sakai S, Hori Y. Road condition estimation for traction control in electric vehicle. Int Symp Ind Electron 1999;2:973–8.

[14] Mokhiamar O, Abe M. Active wheel steering and yaw moment control combination to maximize stability as well as vehicle responsiveness during quick lane change for active vehicle handling safety. J Automobile Eng 2002;216(2):115–24.

[15] Matsumoto N, Kuraoka H, Ohba M. An experimental study on vehicle lateral and yaw motion control. Int Conf Indust Electron, Contr Instrum 1991;1:113–8.

[16] Langson W, Alleyne A. Multivariable bilinear vehicle control using steering and individual wheel torques. Proc Amer Contr Conf 1997;2:1136–40.

[17] Raksincharoensak P, Nagai M, Mouri H. Investigation of automatic path tracking control using four-wheel steering vehicle. Proc Vehicle Electron Conf 2001:73–7.

[18] Hayama R, Nishizaki K, Nakano S, Katou K. The vehicle stability control responsibility improvement using steer-by-wire. Proc Intell Vehicles Symp 2000:596–601.

[19] Fukao T, Miyasaka S, Mori K, Adachi N, Osuka K. Active steering systems based on model reference adaptive non-linear control. Proc Intell Transport Syst 2001:502–7.

[20] Mammar S, Sainte-Marie J, Glaser S. On the use of steer-by-wire systems in lateral driving assistance applications. Int Workshop Robot Human Interactive Commun 2001:487–92.

[21] Yoshimoto K, Tanaka H, Kawakami S. Proposal of driver assistance system for recovering vehicle stability from unstable states by automatic steering. Int Vehicle Electron Conf 1999:514–9.

[22] Sparbert J, Dietmayer K, Streller D. Lane detection and street type classification using laser range images. Proc Intell Transport Syst 2001:454–9.

[23] Kiencke U, Nielsen L. Automotive control systems. Singapore: SAE International; 2000.

[24] Macelloni G, Ruisi R, Pampaloni P, Paloscia S. Microwave radiometry for detecting road ice. Proc Geosci Remote Sensing Symp 1999;2:891–3.

[25] Wollitzer M, Buechler J, Luy JF, Siart U, Schmidhammer E, Detlefsen J, et al. Multifunctional radar sensor for automotive application. IEEE Trans Microwave Theory Tech 1998;46(5):701–8.

[26] Kees N, Detlefsen J. Road surface classification by using a polarimetric coherent radar module at millimeter waves. Proc Telesyst Conf 1994:95–8.

[27] Lewis FL, Abdallah CT, Dawson DM. Control of robot manipulators. New York: Macmillan Publishing Company; 1993.

[28] Mokhiamar O, Abe M. How the four wheels should share forces in an optimum cooperative chassis control. Contr Eng Practice 2006;14(3):295–304.